Biochimica et Biophysica Acta 1838 (2014) 2460–2472

Contents lists available at ScienceDirect

Biochimica et Biophysica Acta

journal homepage: www.elsevier.com/locate/bbamem

Langmuir monolayer studies of the interaction of monoamphiphilic pentacyclic triterpenes with anionic mitochondrial and bacterial membrane phospholipids — Searching for the most active terpene

Marcin Broniatowski *, Michał Flasiński, Katarzyna Zięba, Paweł Miśkowiec

Department of Environmental Chemistry, Faculty of Chemistry, Jagiellonian University, Gronostajowa 3, 30-387 Kraków, Poland

ARTICLE INFO

Article history:
Received 26 January 2014
Received in revised form 3 May 2014
Accepted 5 May 2014
Available online 20 May 2014

Keywords:
Langmuir monolayers
Pentacyclic triterpenes
Cardiolipin
Phosphatidylglycerols
Brewster angle microscopy

ABSTRACT

The interactions of three representative monoamphiphilic pentacyclic triterpenes (PTs) with cardiolipins (CL) and phosphatidylglycerols (PG) extracted from mitochondrial and bacterial membranes were comparatively characterized in binary Langmuir monolayers. The studied terpenes: lupeol, α- and β-amyrin are isomeric compounds known from their broad biological activity. Anticancer and antimicrobial activity of PTs is often correlated with their propensity of being incorporated into mitochondrial and bacterial membranes and their specific interactions with cardiolipins. In our studies on 18 model systems surface pressure (π)–mean molecular area (A) isotherms were registered at five different component proportions in each system. Thermodynamic analysis complemented by in situ Brewster angle microscopy visualization of the investigated mixed films enabled the thorough characterization of the studied systems. It turned out that the investigated terpenes interact more favorably with PG molecules as compared to CLs. For most of the system containing CLs the values of ΔG^{exc} were positive which was interpreted as the ability of the terpenes to disintegrate the membranes rich in CLs. Our results confirmed also that in the light of thermodynamic criterion α-amyrin exhibited the highest potential to disintegrate the CL containing domains in mitochondrial and bacterial membranes. The probable origin of the observed specific interactions between α-amyrin and investigated phospholipids could be explained based on the phenomenon of chiral discrimination. The obtained results were also widely discussed in reference to the biological activity of the studied compounds.

1. Introduction

Secondary metabolites are produced by plants as protective agents against different pathogens and herbivorous animals [1]. They are mainly collected in cuticle of the leaves [2], in bark [3] or in resin, if a plant produces it [4]. Pentacyclic triterpenes (PTs) are the leading group of secondary metabolites found in the tissues of both angiosperms and gymnosperms [1,5]. They are 30 carbon atom isoprenoids (built of 6 isoprene units) which are biosynthesized by plants in the reaction of squalene cyclization [6]. Regarding the structure of the hydrocarbon skeleton the main representatives of PT can be divided into three classes: lupanes, ursanes and oleananes [7] (Scheme 1).

It can be noticed that lupeol and amyrins are isomers of the general formula $C_{30}H_{50}O$. Similarly betulinic, oleanolic and ursolic acids are isomers of the general formula $C_{30}H_{48}O_3$. The compounds occur in nature in their reduced form with the carbon 28 atom in the $-CH_3$ group or in an oxidized form with the carbon 28 atom in the –COOH group. Regarding the cycloalkane skeletons, the lupane system is composed of four cyclohexane rings and one cyclopentane ring (E), all fused in the *trans* conformation [8]. The ursane and oleanane skeletons are built of five cyclohexane rings, which are fused in the *trans* conformation with the exception of C18 carbon atom where the conformation is *cis* [6]. The double bond in ring C between C12 and C13 is typical for the terpenes belonging to these groups. Ursanes and oleananes differ only in the location of one methyl group. Lupanes and ursanes possess 10 chiral carbon atoms in their structure [9], whereas in oleananes the number is reduced to 8.

In some medicinal plants these terpenes occur together [5,10], or one of them may prevail over the others. All the described terpenes here have wide spectrum of pharmaceutical activity [11–13]. All 6 abovementioned terpenes are surface active and can form insoluble monolayers at the water/air interface, but there is one fundamental difference between them. The reduced terpenes: lupeol (Lup), α-amyrin (AMalf) and β-amyrin (AMbet) are simple surfactants with only one polar group (hydroxyl at C3) localized on the terminus of the hydrophobic moiety. On the contrary, the oxidized terpenes are bolaamphiphiles, as they possess two polar groups at opposite termini of the hydrophobic moiety: hydroxyl group at C3 and carboxylic at C17. It is well known from the scientific literature that bolaamphiphiles differ significantly in their surface activity from monoamphiphilic species [14,15]. The same applies to bolaamphiphilic terpenes— they can achieve two

* Corresponding author. Tel.: +48 126646795; fax: +48 126340515.
E-mail address: broniato@chemia.uj.edu.pl (M. Broniatowski).

http://dx.doi.org/10.1016/j.bbamem.2014.05.009
0005-2736/

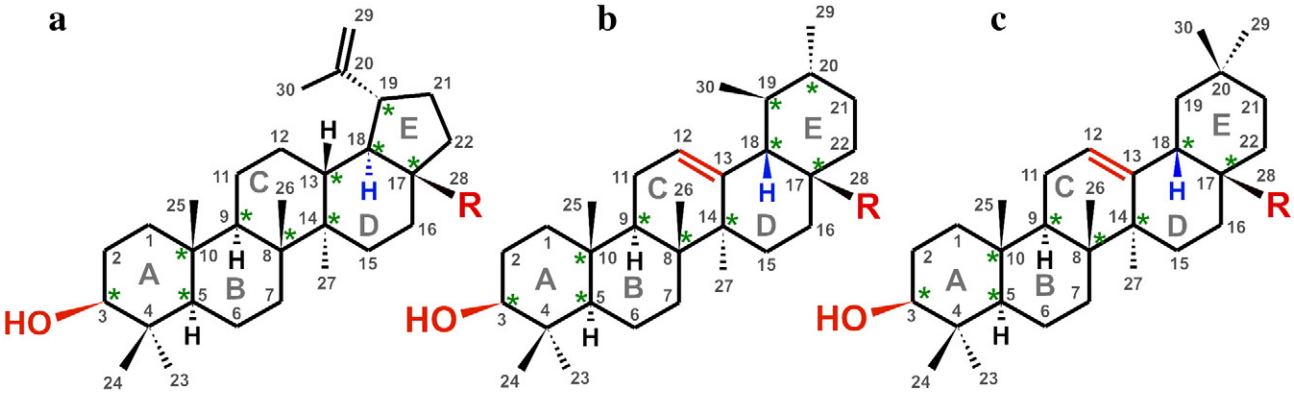

Scheme 1. Structure of the main PTs found in plant material: a) lupane-type, **R = –CH$_3$ lupeol**, R = –COOH betulinic acid; b) ursane-type, **R = –CH$_3$ α-amyrin**, R = –COOH ursolic acid; c) oleanane-type, **R = –CH$_3$ β-amyrin**, R = –COOH oleanolic acid. Black — isoprenoid cycloalkane skeleton, red — substituents and alterations to the ground structure, blue — chiral center differing lupanes from ursanes and oleananes, green asterisks — chiral carbon atoms. Bold font in caption indicates molecules studied in this paper.

different orientations in Langmuir monolayers: upright and tilted which are in equilibrium depending on the surface pressure [16]. As our studies are the first attempt to comprehensively investigate the interactions of PTs with anionic phospholipids it is reasonable to reduce the number of possible terpene orientations in the monolayer. It is guaranteed by the application of monoamphiphilic species which can acquire only the upright orientation at the water/air interface [16]. Therefore, for the experiments presented in this paper we have selected monoamphiphilic terpenes, namely lupeol (Lup), α-amyrin (AMalf) and β-amyrin (AMbet) to investigate their interactions with membrane phospholipids. Lupeol can be treated as a model pentacyclic triterpene, so the scientific literature regarding its biological activity is vast and the properties of this compound were summarized in numerous review articles [11–13]. On the other hand, both properties and biological activity of amyrins are much less discussed in medical, biochemical and pharmaceutical journals. Lupeol was successfully tested as anticancer drug as it was active against different types of cancers [12,17–20]. Amyrins were also tested in cancer therapy; however, the main stress was put on their anti-inflammatory [21,22] and antibacterial properties [23–25]. Lupeol, and amyrins were also active in the therapies of hypercholesterolemia [26,27], asthma [28], diabetes [29], tuberculosis [30] and malaria [31]. Interestingly, apoptotic properties of these terpenes are connected with their specific binding to lipids of tumor cell mitochondrial membranes therefore these molecules are called mitochondrial toxins [17,32]. Similarly, the antibacterial activity of these compounds can also be connected with their interactions with some membrane lipids in both Gram negative and Gram positive bacteria [33]. Both bacterial [34] as well as mitochondrial membranes [35] are characterized by relatively high level of anionic phospholipids, e.g. phosphatidylglycerols and cardiolipins. The latter compounds (cardiolipins (CLs)) are dimeric anionic lipids containing two phosphatidylglycerol moieties, which can be found exclusively in mitochondrial and bacterial membranes. They play important roles in the generation of energy in mitochondria, in the process of the cell division in bacteria and in apoptosis [36]. The beef heart cardiolipin (BHCL), which is the most populated CL in the mitochondria of eukaryotic organisms, contains almost exclusively the linoleic acid rests [37]. It is not the only CL present in animal mitochondria, as in human lymphoblasts dominates tetraoleoyl cardiolipin (TOCL), and the CLs of echinoderms possess mainly polyunsaturated fatty acids. It was also proved that the eukaryotic cardiolipins are symmetrical in respect to the linking glycerol unit [38]. In contrast, bacterial cardiolipins are unsymmetrical and possess typical to bacteria cyclopropylated fatty acid chains or fatty acids with *trans*-unsaturated double bonds [39]. The interactions of CLs with different, mainly amphoteric phospholipids were investigated in Langmuir monolayers [40–42] serving as an efficient technique in the examination of this class of lipids. In these studies mainly BHCL was applied; however, there are also some reports regarding the examination of the not natural tetramiristoyl CL [43].

In our studies we were interested in the interactions of biologically active PTs: lupeol, α and β-amyrins with cardiolipins typical to mitochondrial and bacterial membranes. As representatives of mitochondrial CLs we applied BHCL and TOCL. As bacterial cardiolipin we applied the CL isolated from *Escherichia coli* (ECCL). To have a deeper insight into the studied matter we also applied phosphatidylglycerols (PGs) in our research. The interactions of PTs with PGs are also of interest, taking into consideration that especially in bacterial membranes PGs are the dominating anionic lipids [44,45]. To gain the possibility of the mutual comparison of the experimental results we applied PGs which can be treated as halves of the CL molecules: dilinoleoyl PG (DLPG) as a half of BHCL, dioleoyl PG (DOPG) as a half of TOCL and the main PG isolated from the membrane of *E. coli* (ECPG). In our experiments we investigated the binary Langmuir monolayers formed from the PTs and the anionic lipids. As it can be calculated the combination of 3 terpenes with 6 anionic lipids gave 18 binary surface systems which were studied. All the monolayers within the systems were visualized by Brewster angle microscopy (BAM) upon the film compression. On the basis of the measured surface pressure–mean molecular area isotherms (π–A) we performed thermodynamic analysis calculating the excess free energy of mixing ΔG^{exc} as it is a convenient factor giving insight into the intermolecular interactions in a binary film. In the pharmaceutical studies lupeol and both amyrins together with their oxidized forms (bolaamphiphilic acids) are often tested against tumor cell lines or some pathogens as the plant extract without separation of the components. In our studies we focused on pure, isolated terpenes, as they differ in their structure and chirality between each other, so it is possible that they vary also in their interactions with anionic phospholipids. It was also interesting to compare the results in the pairs CL–PG, to check if there are significant differences in the interactions of PTs with both types of anionic phospholipids.

2. Experimental

2.1. Chemicals

2.1.1. Terpenes

Lupeol (98%), α-amyrin (99%) and β-amyrin (99%) were purchased from Sigma-Aldrich. All the terpenes are analytical standards, purified by HPLC.

2.1.2. Phospholipids

All phospholipids were purchased from Avanti Polar Lipids as chromatographically purified, lyophilized powders. We bought two mitochondrial CLs: beef heart CL (tetralinoleoyl-CL, BHCL) and

tetraoleoyl-CL (TOCL) and one species extracted from *E. coli* (ECCL). We bought also three PG structurally correlated with the investigated CL: dilinoleoyl-PG (DLPG), dioleoyl-PG (DOPG) and PG extracted from *E. coli* (ECPG). The detailed description of the investigated phospholipids together with the structural formulas of ECCL and ECPG can be found in the Supplementary materials as well as on the producer website [46].

2.1.3. Solvents

HPLC grade chloroform (99%) stabilized by ethanol (1%), as well as HPLC grade methanol (99.9%) were bought from Sigma-Aldrich. Ultrapure water of the resistivity ≥18.2 MΩ·cm was produced in our laboratory with the application of the Millipore Synergy System.

2.1.4. Preparation of the surfactant solutions

The powdered samples of the investigated surfactants were weighted on high precision analytical scales (Mettler Toledo) and dissolved in chloroform/methanol (9/1 v/v) mixture in class A 10 cm^3 volumetric flasks. The concentrations of the solutions were 2–3 mg/ml, that is ca. 4–7 · 10^{-4} M for terpenes, ca. 2.5–4 · 10^{-4} M for PGs and ca. 1–2 · 10^{-4} M for CLs. All the stock solutions were stored refrigerated at −20 °C. The mixed binary solutions of the investigated terpenes and phospholipids were prepared in small vials from the stock solutions just before the experiments.

2.1.5. Proportions of the components in the binary monolayers

The dimensions (cross-sections) of the investigated terpenes, PGs and CLs differ between each other. For the terpenes and PGs the molecular areas close to monolayer collapse are comparable (between 40 and 50 $Å^2$/molecule); whereas TOCL and BHCL are 2.5 times bigger (ca. 100–110 $Å^2$/molecule at collapse) and ECCL is 2 times bigger (ca. 85 $Å^2$/molecule at collapse). Therefore, to compare the results it is more reasonable to fix the surface proportions in the binary mixtures and not the molar ratios. Thus, in each binary system we investigated 5 surface proportions: 1:4; 1:2; 1:1; 2:1; and 4:1 (terpene:phospholipid). The recalculation of the applied surface ratios of the components into the mole ratios in the particular binary systems can be found in Table 1.

2.1.6. Langmuir technique

In our experiments we applied the NIMA 301 (NIMA, Coventry, UK) single-barrier Langmuir trough of the nominal area 300 cm^2. The BAM microscopy experiments were performed on KSV (KSV, Helsinki, Finland) double barrier trough of the nominal area 840 cm^2. Surface pressure was monitored with a Wilhelmy-type tensiometer with a filtration paper strap (Whatman, ashless) as the pressure sensor. Surface pressure was acquired with a 1 s time log and every π value is an average of 5 single measurements. The accuracy of the sensor was 0.1 mN/m.

Before an experiment the Langmuir trough was carefully cleaned, after which it was filled with ultrapure water. The appropriate volume of the chloroform/methanol solution of investigated surfactant(s) was deposited at the water/air interface with Hamilton microsyringe. 5 min was left for the spreading solvent evaporation, after which the monolayers were compressed with the barrier speed of 20 cm^2/min. In Langmuir experiments it is also important to fix the number of molecules deposited on the trough, as the isotherm characteristics can depend on this parameter. In our case the investigated molecules differ profoundly in the molecular cross-section so it was more reasonable to fix the constant compression ratio. In all experiments the compression ratio expressed as the quotient of the initial area at the beginning of the compression and the area at monolayer collapse was kept at 4. It means that in the case of the systems with PGs which were expected to collapse approx. at 40 $Å^2$/molecule the compression started always from 160 $Å^2$ and the number of deposited molecules was always constant regardless of X(terpene). In contrast, in the systems with CLs the collapse area is composition dependent, so the compression started always at the molecular area 4 times greater than the collapse area.

All the π–A isotherms were registered at least three times and the average curves were taken for the calculation of the thermodynamic functions. The experimental error of mean molecular area did not exceed 1 $Å^2$/molecule. The subphase temperature was 20 ± 0.1 °C in all the experiments and was controlled by Julabo water circulating bath.

2.1.7. Compression modulus C_S^{-1} and excess free energy of mixing ΔG^{exc}

Compression modulus C_S^{-1} was calculated according to its definition: $C_S^{-1} = -A d\pi / dA$.

The excess free energy of mixing ΔG^{exc} was calculated for binary Langmuir monolayers at a given π value according to its definition [47]:

$$\Delta G^{exc} = \int_0^{\pi} A^{exc} d\pi$$

where A^{exc} is the excess area defined as follows:

$$A^{exc} = A_{12} - (A_1 X_1 - A_2 X_2)$$

where A_{12} is the mean molecular area at a given π value for the binary monolayer, A_1 is the molecular area at the same π for the surfactant1 (one component) monolayer, A_2 is the molecular area at the same π value for the surfactant2 (one component) monolayer. X_1 and X_2 are the mole ratios of surfactant1 and surfactant2 in the binary monolayer ($X_1 + X_2 = 1$).

2.1.8. Brewster angle microscopy

Brewster angle microscopy experiments were performed with ultraBAM instrument (Accurion GmbH, Goettingen, Germany) equipped with a 50 mW laser emitting p-polarized light at a wavelength of 658 nm, a 10× magnification objective, polarizer, analyzer and a CCD camera. The spatial resolution of the BAM was 2 μm. The instrument is coupled with the KSV 2000 Langmuir trough and installed on an antivibration table.

3. Results and discussion

3.1. One-component monolayers

In this paper we present and discuss the data acquired for 18 binary systems, the Langmuir results are vast; therefore, all the π–A isotherms

Table 1
Recalculation of the surface ratios to mole ratios.

Surface ratio (terpene/phospholipid)	Mole ratio of terpene		
	Systems with PGs	Systems with TOCL and BHCL	Systems with ECCL
1:4	0.20	0.38	0.34
1:2	0.34	0.55	0.50
1:1	0.50	0.71	0.66
2:1	0.66	0.83	0.80
4:1	0.80	0.91	0.89

and C_S^{-1}–π curves are shown in the Supplementary material file. However, it seems reasonable to present in the main body of the paper the π–A isotherms registered for one-component monolayers of the investigated surfactants here, as these isotherms are later on used as the references in the ΔG^{exc} calculations.

The investigated terpenes form closely packed monolayers, which according to the C_S^{-1} criterion achieve the solid state (S) of the molecular organization ($C_S^{-1} > 250$ mN/m). The most closely packed is the AMalf monolayer achieving the maximum C_S^{-1} value of c.a. 450 mN/m. It was proved previously with the application of synchrotron radiation diffraction that lupeol monolayer is crystalline even at low surface pressure values [16] and that the molecules are oriented upright at the water/air interface. Similar orientation at the interface and molecular organization can be assumed for α and β amyrins, which are isomers of lupeol and have similar hydrophobic moieties in the molecules. Regarding α and β amyrins a slight difference can be discerned in the course of the π–A isotherms at the beginning of surface pressure rise. In the case of α-amyrin the surface pressure rise is rapid suggesting that the state of α-amyrin monolayer is solid even at low π values. In contrast for β-amyrin film the surface pressure rise is gradual suggesting the transition between liquid condensed and solid states. The described trends here are well visible in the plot of C_S^{-1}–π curves.

In contrast to the investigated terpenes the applied cardiolipins here form expanded monolayers with the C_S^{-1} hardly achieving the limiting value of 100 mN/m; thus the state of the CL monolayers can be described as liquid expanded (LE). The LE state is typical for the monolayers formed on pure aqueous subphase at room temperature by surfactant possessing double bonds in their fatty acid chains. To the best of our knowledge the π–A isotherm of TOCL has not been published previously; whereas, as it was mentioned in the Introduction section, the π–A isotherm of BHCL was published many times and our results are in accordance with these published previously [42,48,49]. ECCL also contains unsaturated chains and the cyclopropylated fatty acid chain, so it also cannot achieve higher order than the LE state. As it was expected the characteristic of the PGs monolayers was similar to the above described CLs. It can be noticed in Fig. 1, that the π–A isotherms of ECCL and ECPG are shifted towards lower mean molecular areas. It is the result of the presence of the palmitoyl acyl chain in the hydrophobic moiety of both lipids. Palmitoic acid is saturated, so the effective cross-section of ECCL and ECPG is smaller than in the case of the other anionic phospholipids investigated here, and the isotherms are systematically shifted. ECCL possesses also unsaturated chains in its hydrophobic moiety, so the presence of palmitoyl rests does not find any manifestation in the C_S^{-1}–π curves. In contrast ECPG do not posses unsaturated chains in its structure, but one saturated and one cyclopropylated, so its monolayers are more condensed as compared to DOPG and DLPG.

All the monolayers of the investigated terpenes, CLs and PGs were visualized by the Brewster angle microscopy. All the monolayers are homogenous and no condensed domains or other distinct structures were observed between the beginning of surface pressure rise and the monolayer collapse. The BAM images for lupeol were published previously [16] and both amyrins behave similarly. Generally, the terpene films are homogenous upon their compression. They collapse by surface crystallization — suddenly a large number of small 3D crystallites, visible as bright points appear in the BAM image.

3.2. Binary systems containing the investigated terpenes and TOCL or DOPG

TOCL has the advantage as compared to the other two CLs that it is synthetic, possesses exclusively the oleic acid fatty acid chains, so the terpene/TOCL systems are really binary, there are no minor amounts of other cardiolipins making the systems multicomponent — as it can be in the case of BHCL or ECCL. Below in Fig. 2 the ΔG^{exc}-X(terpene) dependences for the six systems with TOCL and DOPG are presented.

As it is visible in Fig. 2 there are profound differences between the systems containing TOCL and DOPG. In systems with TOCL ΔG^{exc} has the positive sign (with the exception of the 0.38 and 0.55 mole ratios in the system AMbet/TOCL where it is close to 0 or negative). On the contrary, in systems with DOPG for both amyrins ΔG^{exc} is negative (significantly at higher surface pressure) or close to 0 in the system Lup/DOPG. Apart from the ΔG^{exc} calculation we extracted from the π–A isotherms the collapse pressures (π_{coll}) and from the C_S^{-1}–π curves the maximal values and plotted them versus X(terpene). The π_{coll}-X dependences are important in the discussion of mutual miscibility in a

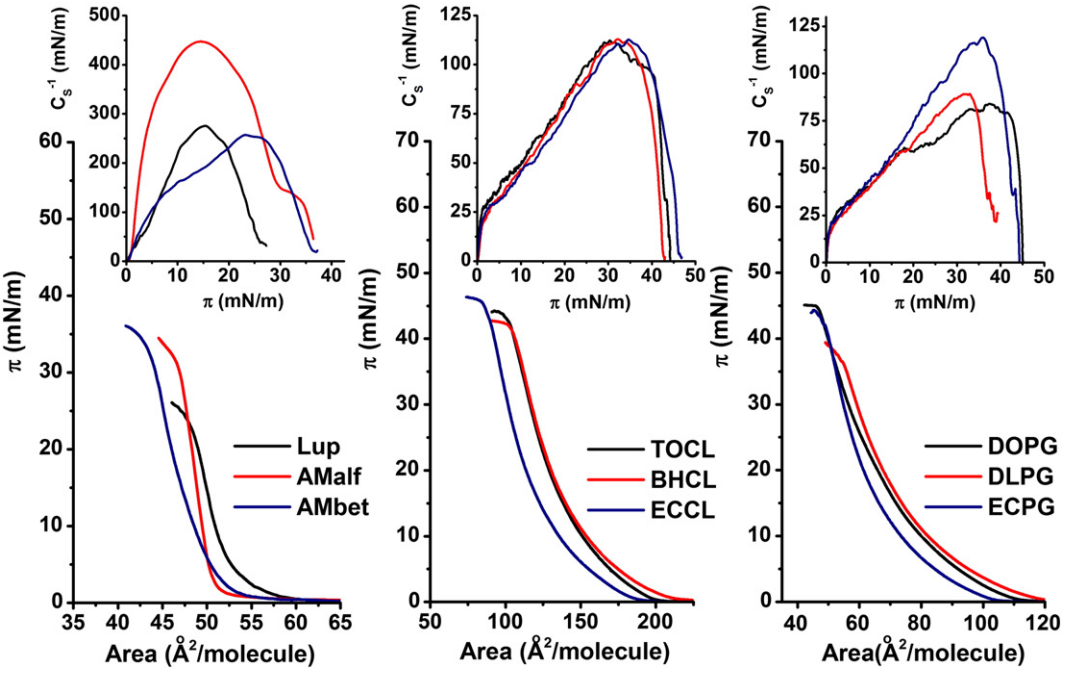

Fig. 1. π–A isotherms and C_S^{-1}–π curves (insets) registered for one-component monolayers of the investigated terpenes (left panel), cardiolipins (middle panel) and phosphatidylglycerols (right panel).

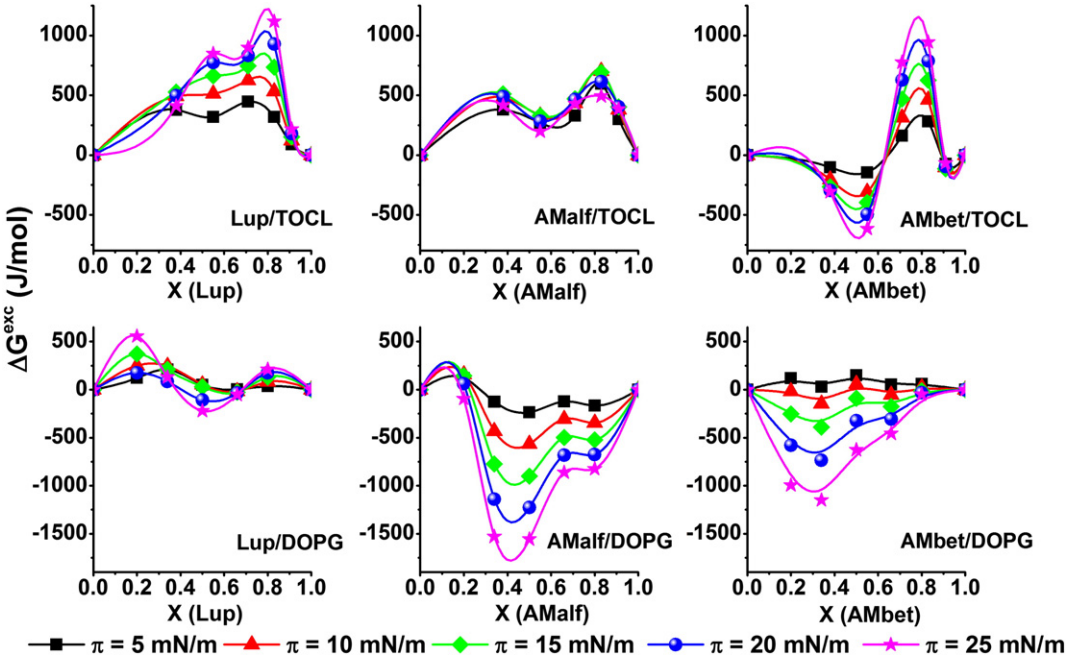

Fig. 2. ΔG^{exc}-X(terpene) dependences for the systems with TOCL and DOPG. The points are exact values calculated for the given π value, the curves are only guidelines for the eye underlining the trend in a binary monolayer.

binary monolayer; whereas, the C_S^{-1}max-X dependences illustrate the effect of the component ratio on the monolayer condensation.

It can be noticed that the collapse pressure in all the discussed systems depends on the mutual proportion of its components. The collapse pressures of the phospholipids' monolayers are higher than the collapse pressures of the terpenes' films. With increasing X(terpene) a decrease of π_{coll} can be observed. If in a binary monolayer only one collapse pressure can be observed, and if it is composition depended, it can be inferred that both surfactants forming the monolayer are mutually miscible. It would be of interest to discuss together the ΔG^{exc}-X(terpene) and π_{coll}-X(terpene) dependences as on the first glance they are mutually contradictory. It should be reminded that the sign and value of ΔG^{exc} are not direct indicators of phase separation/mutual miscibility in binary Langmuir monolayers. The negative sign indicates that the interactions between two different surfactants in binary monolayer are more beneficial (attractive) than the interactions between the same molecules in one-component film. Thus from the negative sign of ΔG^{exc} it can be inferred that the two components of a binary film should be miscible. For positive sign of ΔG^{exc} the interpretation can generally be vice versa. However, it should be underlined that positive sign of ΔG^{exc}, even if correlated with significant ΔG^{exc} value, does not necessarily indicate phase separation in a given system. It indicates directly only the fact that the interactions between two different surfactants are less attractive than between the same molecules in one-component films. The interactions can be less attractive, but the film-forming molecules can still be miscible. Therefore, for the characterization of binary and multicomponent films different mutually independent methods should be applied. The comparison of the results collected in such independent experiments leads to the elucidation of a phase diagram of the investigated system in given thermodynamic conditions. In the case of our studies BAM measurements can be of help as the additional, independent physicochemical method. Additional data about the investigated systems can also be inferred from the C_S^{-1}max-X(terpene) plots. It can be seen that up to the X(terpene) = 0.71 (1:1 surface proportion) the presence of terpene has virtually no effect on TOCL monolayer condensation expressed in the C_S^{-1}max values scale. In contrast the presence of terpene in DOPG up to the 1:1 surface proportion (X(terpene) = 0.66) has a destabilizing effect on the monolayer, which is more expanded; thus, less organized than the pure DOPG monolayer. The condensing effect can be seen in the systems with TOCL and DOPG only in the monolayers in which terpene dominates (2:1 and 4:1 surface proportions).

All the monolayers were visualized by BAM upon the film compression. Similarly to pure components most of the binary monolayers were homogenous till collapse. There were; however, such compound proportions in particular systems where interesting textures were observed. These cases are illustrated in Fig. 4.

The above presented BAM images can be divided on two categories: condense 2D domain formation (panels: a, b, c, f, h, i) and 3D domain separation (d, e g, j, k, l). 2D domains were observed in the system Lup/TOCL at X(lup) = 0.71 (a) and X(lup) = 0.83 (b). The domains were quite long and had ragged edges. Such domains were not observed in the systems with amyrins. In contrast at the lowest AMalf or AMbet proportion (X(AM) = 0.38) circular condensed domains were present in the BAM images (panels c and f). They were much smaller in the case of AMbet than in the monolayer containing AMalf. The phenomenon of phase separation was observed in the systems with amyrins at high terpene concentration (panels d, e, g). However, the three panels, mentioned in the bracket, visualize two different kinds of phase separation. In panel e condensed gray 2D phase separated from the expanded darker regions of the monolayer; whereas in panels d and g small crystallites of a 3D phase separated from the investigated films. Regarding the systems with DOPG 2D domain formation is depicted in panels h and i and phase separation of 3D domains in panels j, k and l. In the system Lup/DOPG at lower X(Lup) small circular domains of the condensed phase are present in the BAM images, whereas at X(Lup) = 0.66 long grass-leaf domains were observed. Phase separation of 3D domains was observed for the systems with amyrins at low or moderate terpene proportion at surface pressures ranging from 15 to 20 mN/m.

As far as the phase separation of 3D domains is concerned, the most important difference between the systems with TOCL and DOPG is connected with the amyrin concentration at which the separation phenomenon was observed, as in the former case the concentrations were high and in the latter low. We tried to correlate the BAM images and the elasticity of the monolayers looking for the manifestation of the phase transitions in the course of C_S^{-1}–π plots (Fig. 5).

In the case of the systems AMalf/DOPG and AMbet/DOPG at the above mentioned amyrin proportions there is a minimum in the course of the C_S^{-1}-X(terpene) plot. The values of $C_S^{-1}$are lower than 100 mN/m,

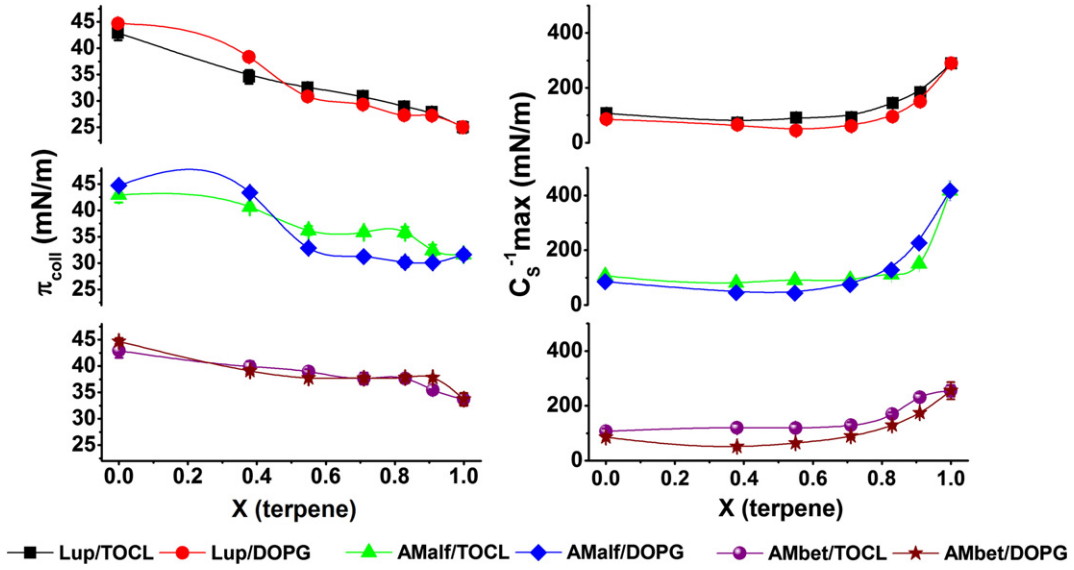

Fig. 3. π_{coll}-X(terpene) (left panel) and C_S^{-1}max-X(terpene) (right panel) dependences.

indicating that in the whole range of compression the monolayers are liquid expanded. Therefore, the phase transition manifested as the minimum is connected not with a transition leading to a more organized phase but with expulsion of a 3D phase from the dominating phospholipid liquid-expanded film. We do not show here the C_S^{-1}–π curves for the systems with TOCL as there were no manifestations of a 2D–3D transitions different than film collapse observed in the course of these curves (these curves are available in Supporting materials). The TOCL monolayer was liquid expanded and TOCL did not tend to aggregate in its films at the water/air interface, so the 3D domains observed at high amyrin proportions should originate from the expulsion of amyrin from the systems. It was also of interest to correlate the ΔG^{exc}-X(terpene) plots with the BAM images in which phase separation was observed. In the system AMalf/TOCL the sign of ΔG^{exc} was positive for all component proportions and the highest values were observed for the highest AMalf proportions. Such trends in the ΔG^{exc}-X(Amalf) curves make phase separation probable and it was corroborated in certain thermodynamic conditions by BAM images. In the system AMalf/DOPG phase separation was observed only at X(AMalf) = 0.2. Interestingly, only for this AMalf mole ratio the values of ΔG^{exc} were positive. In the system AMbet/DOPG the values of ΔG^{exc} were negative indicating that the interactions between AMbet and

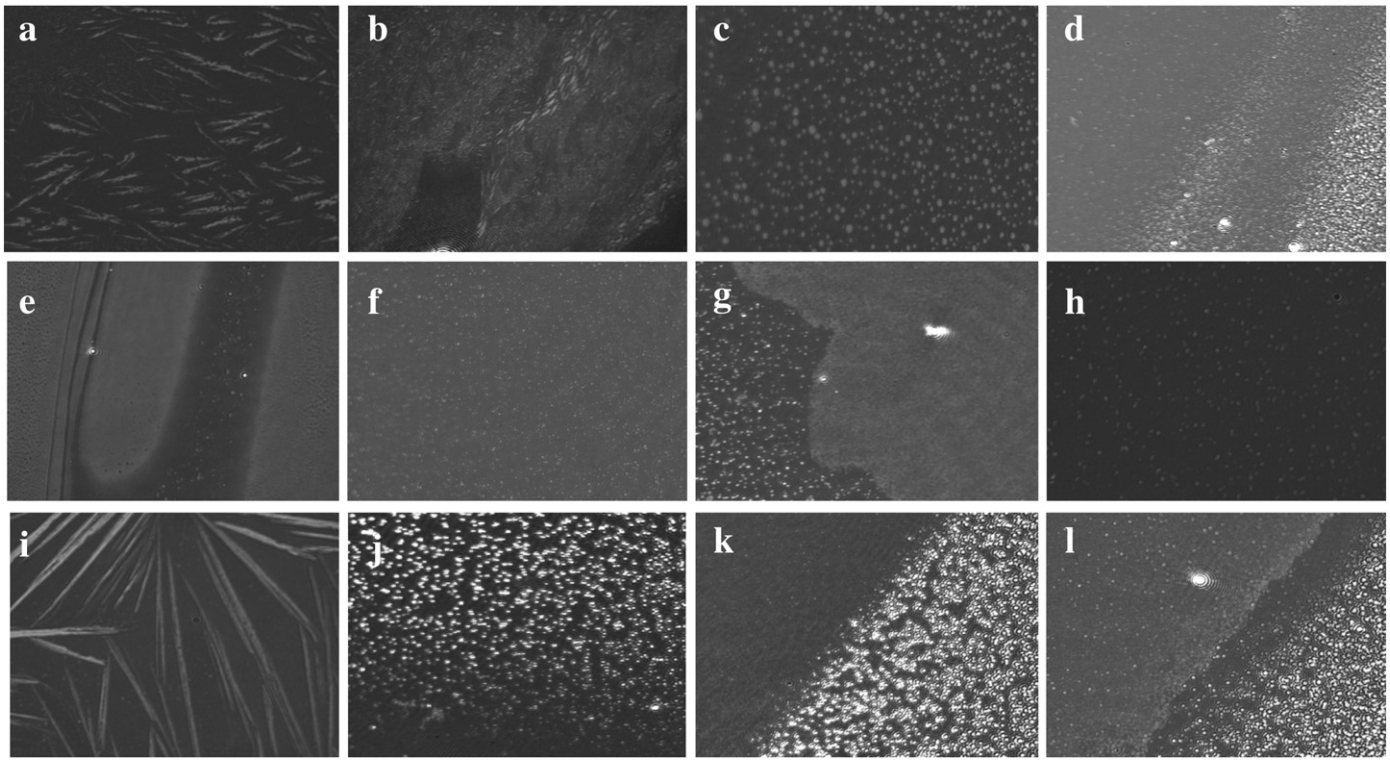

Fig. 4. Selected BAM images for the systems with TOCL (a–g) and DOPG (h–l). a) X(lup) = 0.71, π = 20 mN/m, b) X(lup) = 0.83, π = 7.3 mN/m, c) X(AMalf) = 0.38, π = 11.7 mN/m, d) X(AMalf) = 0.83, π = 23 mN/m, e) X(AMalf) = 0.91, π = 11 mN/m, f) X(AMbet) = 0.38, π = 11.7 mN/m, g) X(AMbet) = 0.71, π = 14.7 mN/m, h) X(Lup) = 0.2, π = 3.1 mN/m, i) X(Lup) = 0.66, π = 4.8 mN/m, j) X(AMalf) = 0.2, π = 15 mN/m, k) X(AMbet) = 0.2, π = 16.8 mN/m, l) X(AMbet) = 0.5, π = 21.3 mN/m.

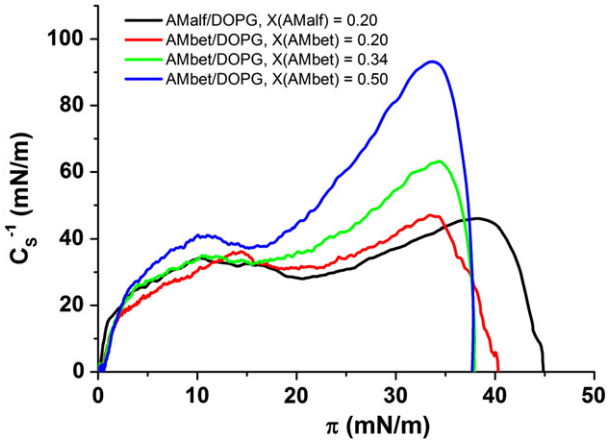

Fig. 5. Compression modulus (C_S^{-1}–π) plots for selected mixtures of AMalf and AMbet with DOPG.

DOPG molecules are energetically beneficial. On the other hand phase separation of 3D domains was observed at certain thermodynamic conditions. Similar behavior was observed for some model Langmuir monolayers composed of phospholipids and a plant sterol or stanol [50,51]. Generally, it is believed that such monolayers can absorb only limited amount of the steroid/terpenoid compound. So, the excess steroid molecules are expelled from the monolayer as 3D crystallites [50,51]. ΔG^{exc} is calculated for 2D monolayers, so the ΔG^{exc}-X(terpene) plot cannot monitor the occurrence of such crystallites. Thus, in our experiments such 3D domains could occur in both the systems with negative ΔG^{exc} as well as those characterized by positive sign of ΔG^{exc}. The aim of our model studies was to discriminate over the investigated terpenes and indicate which of them has the highest potential to disintegrate the CL-reach domains. The sign of ΔG^{exc} was positive for all the systems containing TOCL and negative or close to 0 for those with DOPG, so, on the basis of this criterion, it is evident that the investigated PT can more probably disintegrate the CL-rich domains than those rich in PG. From the three investigated terpenes here lupeol has the highest positive ΔG^{exc} values, so in the interaction with TOCL it should be considered as the compound of choice. TOCL is the main CL only in lymphoblast and not in other tissues [36], so lupeol can be effective in the therapies of some kinds of leukemia, but for the other kinds of cancers the results with BHCL are more representative.

3.3. Binary systems composed of the investigated terpenes and BHCL or DLPG

The ΔG^{exc}-X(terpene) plots in the systems with BHCL (Fig. 6) are similar to the previously discussed for TOCL as far as the sign of ΔG^{exc} is concerned but in contrast to the previously discussed systems the values are much higher for amyrins than for lupeol. There is a slight difference between the systems AMbet/TOCL and AMbet/BHCL, as in the former the values of ΔG^{exc} at X(AMbet) = 0.38 and 0.55 are slightly negative, while in the latter all values are positive (or close to 0 for X(AMbet) = 0.38). The results for the mixtures of amyrins with DOPG and DLPG are practically identical; whereas there are profound differences between the systems Lup/DOPG and Lup/DLPG. In the former case the ΔG^{exc} values oscillate around 0; whereas in the latter they are significantly negative. Regarding the π_{coll}-X(terpene) and C_S^{-1}-X(terpene) plots the trends observed are virtually identical as visible in Fig. 3. Therefore, the plot was shifted to the Supporting materials (S. Fig. 1) and the description of Fig. 3 is also valid here.

As far as BAM images are concerned most of the monolayers within the investigated systems were homogenous as in the previously discussed systems with TOCL and DOPG. The most distinctive exceptions are illustrated by the representative BAM images in Fig. 7.

In the system Lup/BHCL at the lowest lupeol surface proportion (1:4, X(Lup) = 0.38) very long "grass-leaf" domains are visible in the photo. Interestingly such domains were not present at X(Lup) = 0.55, instead small circular domains were visible in the monolayer, as in the left-hand side of panel b. At X(Lup) = 0.71 two kinds of condensed domains were observed — small circular and more bright similar to that observed at X(Lup) = 0.38; thus, two separated phases are present in this system at that proportion of the components. At higher lupeol concentrations the monolayers were homogenous. In the systems AMalf/BHCL and AMalf/TOCL condensed domains were observed only at the lowest amyrin proportion (X = 0.38). In the former system the domains were circular and similar in size (panel c); whereas in the latter the domains were much smaller (photo not shown). In contrast to the system Lup/BHCL at higher amyrin concentrations the monolayers in both systems were homogeneous. Similarly in both systems containing amyrins and DLPG all monolayers were homogenous. Once again lupeol differs from amyrins in the interactions with the investigated phospholipids. Only the monolayer at X(Lup) = 0.8 was homogenous, at other lupeol mole ratios the films developed interesting textures upon compression. At the lowest lupeol proportion small circular domains were present in the monolayer (panel d). At the following X(Lup) = 0.34 such domains were also present, but were less numerous. At X(Lup) = 0.5 the "grass-leaf" texture developed (panel e). Such domains were also visible at X(Lup) = 0.66. It should be underlined that, in contrast to the systems with DOPG and TOCL, the expulsion of 3D domains from the mixed films was not observed at any surface proportion of the components.

At the beginning of the discussion of the results obtained for the systems with BHCL and DLPG it should be once again underlined that tetralinoleoyl CL is the main species of CL in prokaryotic mitochondria [37], so the results for BHCL are more representative than those collected for TOCL. Here, similar to the systems with TOCL, the sign of ΔG^{exc} is positive in all systems containing BHCL. In the systems with TOCL the highest values of ΔG^{exc} were observed for its mixtures with lupeol. In contrast in systems with BHCL the ΔG^{exc} values are much higher in the mixtures with amyrins than with lupeol. The highest values were observed for AMalf, so following the criterion of ΔG^{exc} this compound has the highest potential to disintegrate the membrane domains containing BHCL. Regarding the BAM images, similar to previously discussed systems condensed circular domains are visible at the lowest AM proportion. Taking into consideration that the pure monolayers of amyrins and BHCL are homogenous, the presence of such domains proves that even small amount of amyrins incorporated into the CL-reach domain can lead to significant alterations of its function. The ΔG^{exc} was smaller for lupeol than for amyrins, but it is visible in BAM images that the incorporation of lupeol in the anionic phospholipid monolayer causes the most significant alterations in model membrane morphology.

3.4. Binary systems composed of the investigated terpenes and E. coli lipids ECCL or ECPG

The anionic phospholipids of *E. coli* differ significantly in the structure of the fatty acid chains from eukaryotic phospholipids, so it is not surprising that the ΔG^{exc}-X(terpene) plots vary profoundly from the previous discussion. At first glance it is visible in Fig. 8 that there are significant differences between lupeol, α-amyrin and β-amyrin. On the other hand there are virtually no qualitative differences between ECCL and ECPG which also differentiates the systems with *E. coli* lipids from the previous discussion. For the systems with lupeol the sign of ΔG^{exc} is negative, the absolute values are approximately two times greater in the system with ECCL than with ECPG. In the systems with AMalf the sign of ΔG^{exc} is positive and the absolute values are ca. 4 times greater in the system with ECCL than with ECPG. In the system AMbet/ECCL ΔG^{exc} has negative sign for the lowest amyrin proportion, but for the higher proportions ΔG^{exc} values are positive, but approximately 3 times lower than in the system with AMalf. In the system

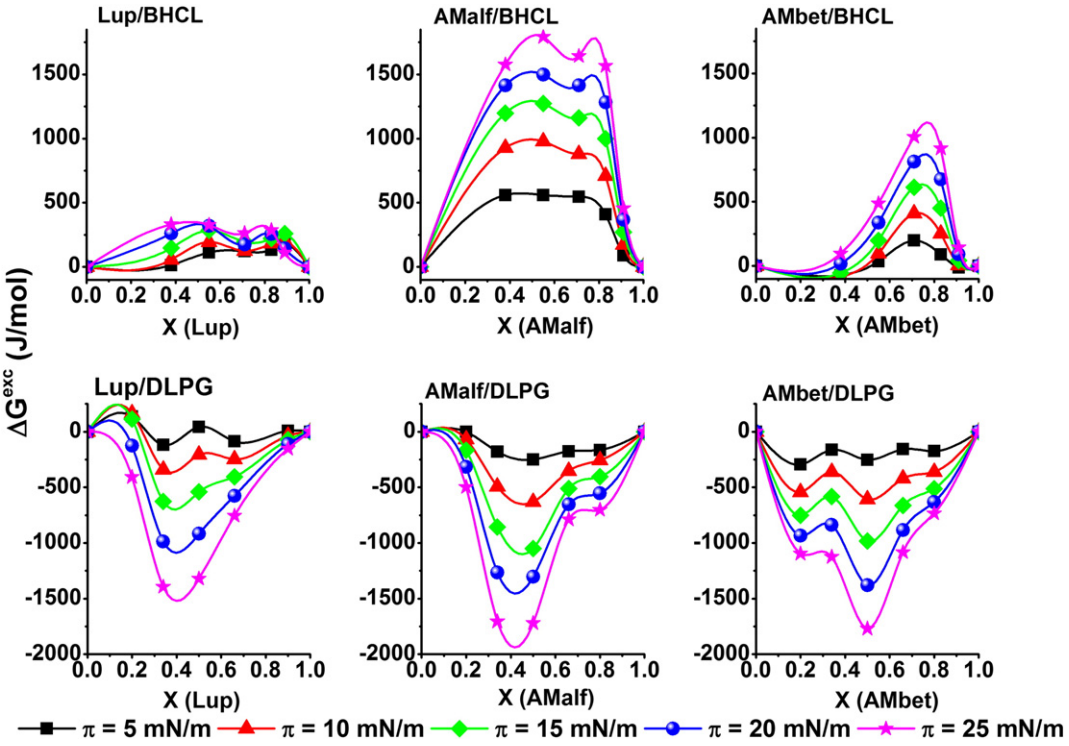

Fig. 6. ΔG^{exc}-X(terpene) dependences for the systems with BHCL and DLPG. The points are exact values calculated for the given π value, the curves are only guidelines for the eye underlining the trend in a binary monolayer.

AMbet/ECPG ΔG^{exc} oscillates around 0 or acquires negative values for higher surface pressures. Only for the highest X(AMbet) = 0.8 ΔG^{exc} acquires positive values.

Similar to the other systems the π_{coll}-X(terpene) and maximal value C_S^{-1}-X(terpene) plots were prepared and are presented in Fig. 9.

With the increasing X(terpene) the collapse pressures diminish quite linearly from the highest value observed for the pure anionic phospholipid to the lowest value observed for the pure terpene monolayer. Such trend in the π_{coll}-X(terpene) dependence proves the mutual miscibility of the components in all the investigated binary systems.

Regarding the C_S^{-1}max-X(terpene) plots it can be noticed that the addition of the terpene exerts expansive effect on the ECPG monolayer and leads to the increase of disorder in these systems. This trend is much more visible for amyrins, especially AMbet than for lupeol. The mixed monolayers composed of the investigated terpenes and ECCL have similar condensation as pure ECCL monolayers.

All the monolayers in the discussed systems were visualized upon compression. Similar to the previously discussed systems, most of the investigated monolayers were homogeneous in BAM images from the beginning of film compression till the collapse. The exceptions from this rule are gathered in Fig. 10.

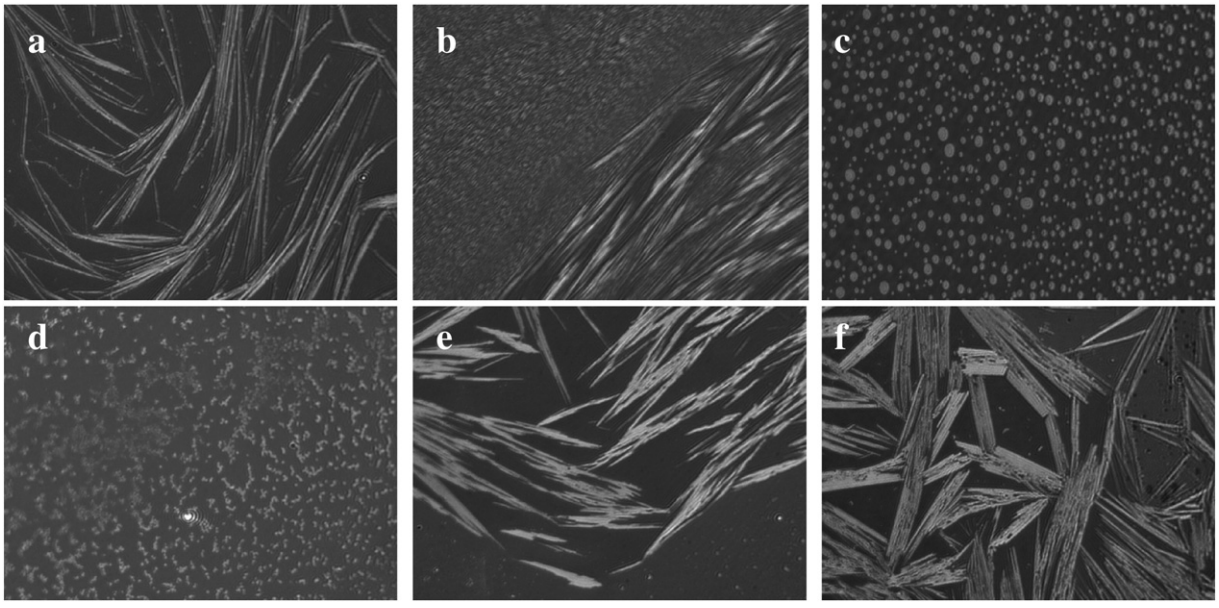

Fig. 7. Representative BAM images for the systems with BHCL (a–c) and with DLPG (d–f): a) X(Lup) = 0.38, π = 16.5 mN/m, b) X(Lup) = 0.71, π = 10 mN/m, c) X(AMalf) = 0.38, π = 12.3 mN/m, d) X(Lup) = 0.2, π = 17.6 mN/m, e) X(Lup) = 0.5, π = 8.8 mN/m, f) X(Lup) = 0.66, π = 2.7 mN/m.

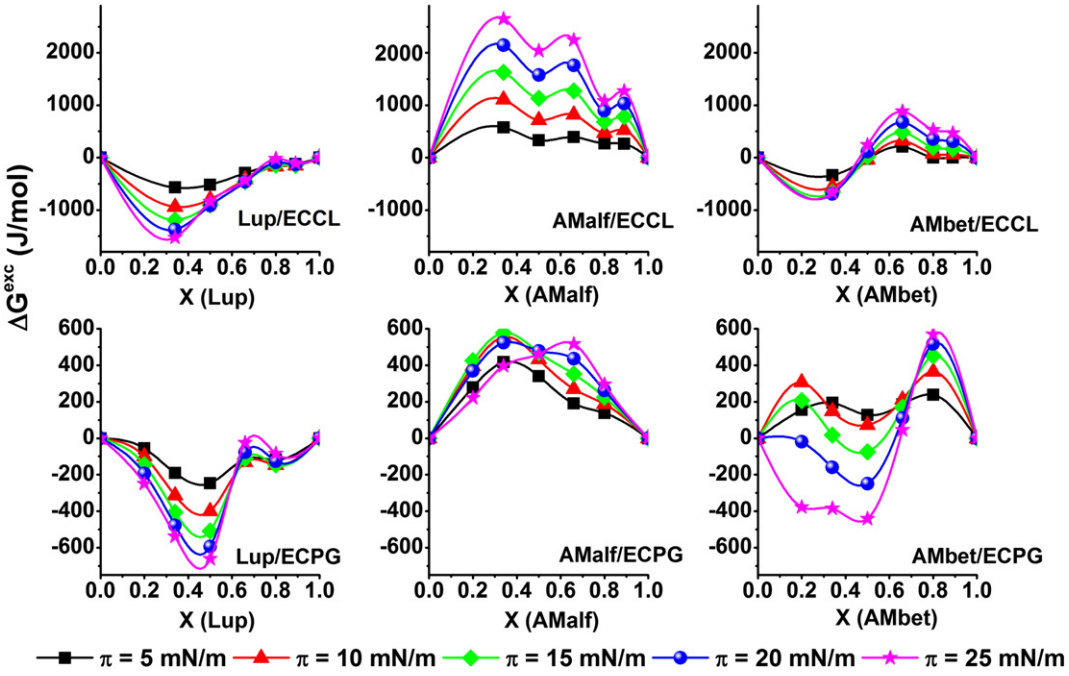

Fig. 8. ΔG^{exc}-X(terpene) dependences for the systems with ECCL and ECPG. The points are exact values calculated for the given π value, the curves are only guidelines for the eye underlining the trend in a binary monolayer.

The photos in Fig. 10 can be divided on three categories: images illustrating the separation of 3D domains (panels a, c, d, l), images illustrating phase separation of 2D phases (f, g, i) and images illustrating the presence of small condense 2D domains (b, e, h, j, k). In the system Lup/ECCL all the monolayers were homogenous for low and moderate lupeol proportions. At X(Lup) = 0.8 the monolayer was homogenous till the surface pressure of 14 mN/, where 3D domains were expelled from the monolayer (panel a). Interestingly, at the highest lupeol mole ratio of 0.89 no 3D domains appeared before the monolayer collapse. The appearance of 3D domains at the particular terpene surface proportion of 0.8 can be explained in the same way as in the previously cited papers regarding the interactions of phospholipids with steroids [50,51]. Generally, the interactions of lupeol with ECCL are energetically favorable as it is visible in the ΔG^{exc}-X(Lup) plot (Fig. 8); however, in such systems at some sterol (terpene)/phospholipid proportion the excess sterol (terpene) can be expelled from the monolayer at particular thermodynamic conditions. Regarding the systems containing amyrins and ECCL, despite positive values of ΔG^{exc}, the BAM images recorded for them were homogeneous for most compositions. Phase separation of excess terpene in the form of small 3D domains was only observed at high amyrin proportions (panels c and d). Interestingly, in the system AMalf/ECCL at the lowest X(AMalf) of 0.34 small condensed domains was present in the monolayer (panel b). Similar domains but less numerable and even smaller (at the limit of the microscope resolution) were also observed in the system AMbet/ECCL at X(AMbet) = 0.34 (photo not shown).

The monolayers in the system Lup/ECPG were homogenous at X(Lup) = 0.2 and 0.34, whereas at X(Lup) = 0.5 multiple small condense 2D domains formed at higher surface pressures (panel e). At the monolayers in which lupeol dominated over ECPG (X(Lup) = 0.66

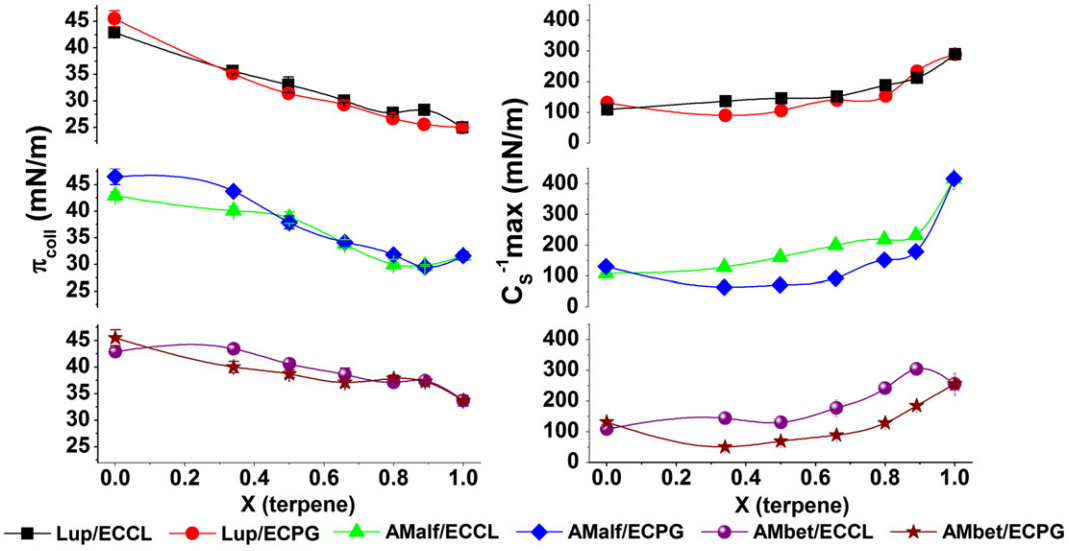

Fig. 9. π_{coll}-X(terpene) (left panel) and C_S^{-1}max-X(terpene) (right panel) dependences.

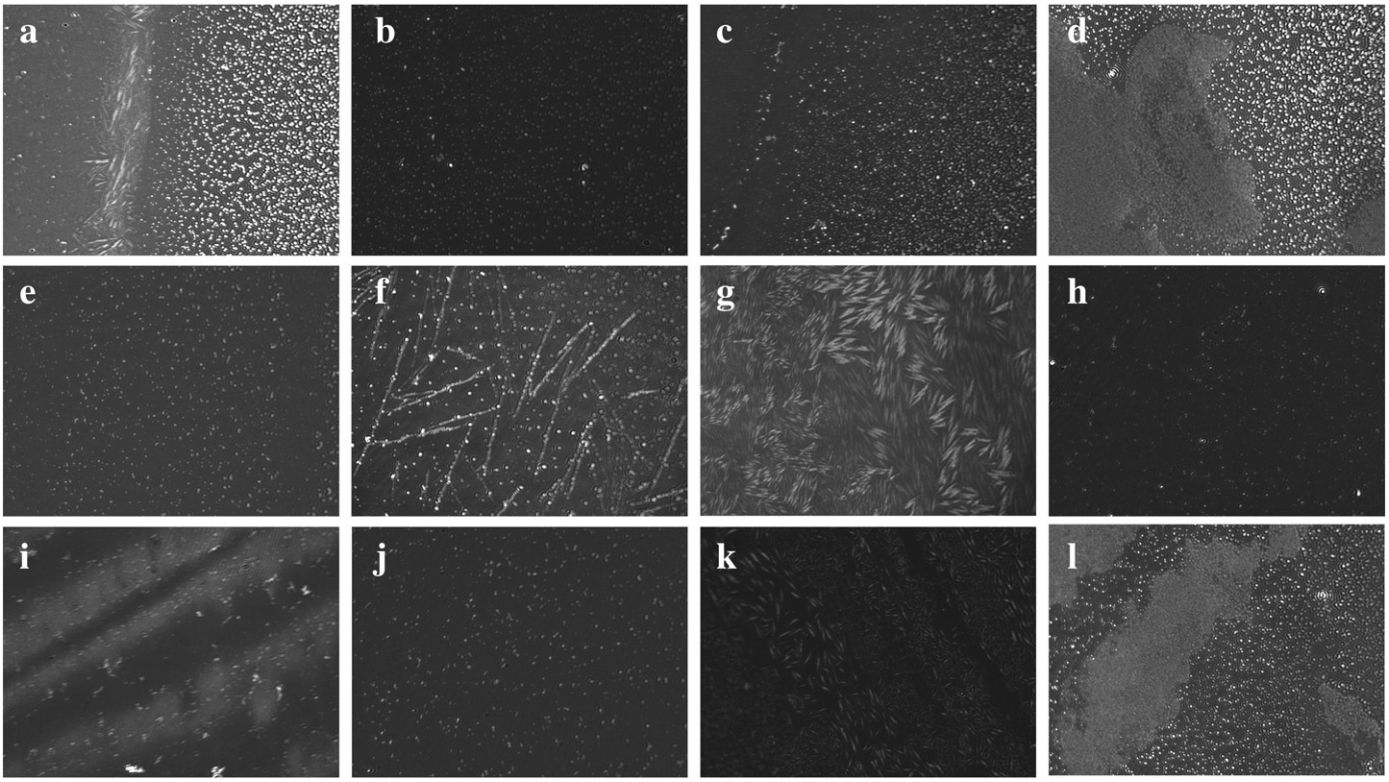

Fig. 10. Representative BAM images for the systems with ECCL (a–d) and ECPG (e–l): a) X(Lup) = 0.8, π = 14 mN/m; b) X(AMalf) = 0.34, π = 18 mN/m; c) X(AMalf) = 0.89, π = 22 mN/m; d) X(AMbet) = 0.8, π = 16 mN/m; e) X(Lup) = 0.5, π = 20 mN/m; f) X(Lup) = 0.66, π = 6.5 mN/m; g) X(Lup) = 0.8, π = 7 mN/m; h) X(AMalf) = 0.2, π = 8.3 mN/m; i) X(AMalf) = 0.8, π = 8 mN/m; j) X(AMbet) = 0.2, π = 10 mN/m; k) X(AMbet) = 0.34, π = 4 mN/m; l) X(AMbet) = 0.8, π = 16.5 mN/m.

and 0.8) phase separation of 2D condense domains from less organized monolayer regions was observed (panels f and g). Such behavior is in accordance with ΔG^{exc}-X(Lup) dependences calculated for this system (Fig. 8). As far as the systems containing amyrins and ECPG are concerned, small condensed domains were observed, even at low surface pressures, for the monolayers containing low amyrin proportion (panels h, j, k). The monolayers containing higher amyrin proportion were homogenous till their collapse. Only at the highest amyrin proportion of 0.8 for both amyrins phase separation of terpene-rich 3D domains was observed.

A very interesting fact observed in the BAM images is the formation of small condensed domains observed in the systems containing both amyrins and ECCL at the lowest terpene mole ratio of 0.34 and in the systems containing amyrins and ECPG at the amyrin ratios of 0.2 and 0.34. Amyrins are antimicrobial agents so any changes in the morphology of the monolayers of *E. coli* lipids correlated with the incorporation of amyrins are of interest here. The occurrence of such domains can be treated here as a factor destabilizing the structure of the membrane. To have a deeper insight into this phenomenon we returned to the π–A isotherms recorded for the discussed monolayers here and focused our attention to their elasticity. The corresponding compression modulus (C_S^{-1})- surface pressure π curves are illustrated in Fig. 11.

Regarding the systems with ECCL, there is an inflection point in the C_S^{-1}–π plots observed for both amyrins between 5 and 10 mN/m. These π values correspond with the surface pressures at which first condensed domains appear in BAM images. Similar transition can be observed in the course of the C_S^{-1}–π curves in the systems with ECPG. However, here the plateau in the modulus plots is very long and the maximal C_S^{-1} values are low remaining in the range typical for the liquid expanded state. On the other hand, it can be seen in Fig. 1 that the elasticity characteristics of the pure one-component monolayers of ECCL and ECPG are very similar, as the C_S^{-1}–π curves in both cases are virtually identical. Therefore, we observe here a discriminating effect of amyrins over both *E. coli* phospholipids. The ΔG^{exc} values are higher in the systems with ECCL, but taking into consideration, the lowering of monolayer condensation, amyrins have higher propensity to disorganize the monolayer of bacterial PG than of bacterial CL. A question regarding the character of the domains observed in the BAM photos can be also asked. It seems that in the light of the C_S^{-1}–π curves these domains can differ in their origin. In the case of ECCL the appearance of the domains can be connected with the partial component segregation;

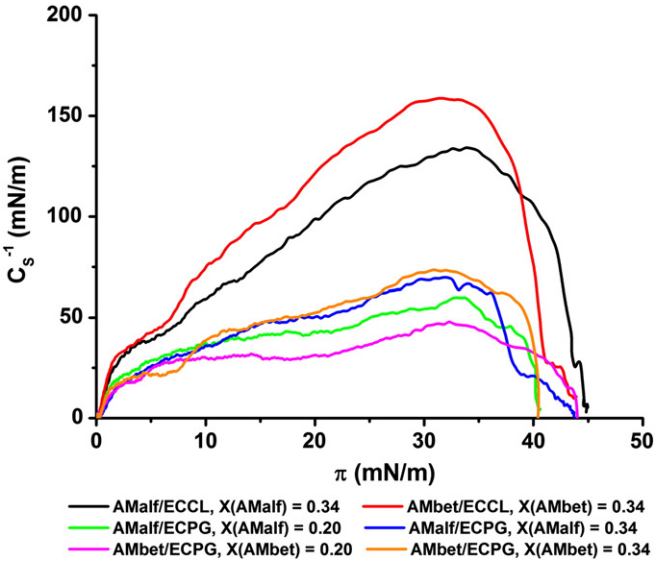

Fig. 11. C_S^{-1}–π dependences for the binary systems containing amyrins and *E. coli* lipids for the lowest proportions of amyrins.

whereas in the case of ECPG the segregation is rather connected with the expulsion of amyrin domains from the mixed film. Such interpretation explains the observed values of C_S^{-1}: in the systems with ECCL they are higher than for pure ECCL monolayer and in the systems with ECPG they are significantly lower than for pure ECPG monolayer in the same experimental conditions.

The discriminating effect of *E. coli* lipids over the investigated terpenes is one of the most important results obtained in these studies. In the above fragments regarding the mixtures of the investigated terpenes with mitochondrial anionic lipids the results for all these terpenes were qualitatively similar, as far as the criterion of the sign of ΔG^{exc} was concerned. Moreover, the data varied between CLs and PGs, as for CLs the sign was positive and for PGs negative. Here the results depend on the applied terpene but are qualitatively similar for ECCL and ECPG as far as the ΔG^{exc}-X(terpene) and π_{coll}-X(terpene) plots are concerned. On the other hand, the C_S^{-1}max-X(terpene) plots differentiate both classes of *E. coli* lipids as it was indicated in Fig. 11. The differences in the condensation of the mixed terpene/*E. coli* phospholipid films can also be explained taking into consideration the composition of the hydrophobic moieties of both lipids. ECPG does not contain unsaturated acyl chains, only the saturated palmitoyl and cyclopropylated-heptadecanoic rests. Thus, the monolayers of ECPG are better organized than the ECCL films and the addition of PT can have an expanding effect on them. Such an effect is not observed in the case on the less organized ECCL monolayers.

Regarding the discriminating effect of *E. coli* phospholipids, for lupeol the sign of ΔG^{exc} is negative, for AMalf the sign is positive, whereas in the mixtures with AMbet ΔG^{exc} changes its sign. Two factors can be of importance in the interpretation of the interactions of the investigated terpenes with *E. coli* phospholipids. The first is their interaction with the cyclo-17:0 fatty acid rest and the second the problem of chiral recognition. The presence of cyclopropane ring is typical for bacterial membrane phospholipids [52–54]. There are different hypotheses about its function, but there is an agreement that the presence of cyclopropane ring instead of a double bond is strictly connected with the adaptation of bacterial cell to its environment [54]. The cyclo-17:0 chain with the cyclopropane ring located in the middle is present both in ECCL and ECPG. It is an additional steric hindrance which can profoundly affect the interaction of the investigated terpenes with *E. coli* phospholipids. The distribution of methyl groups along the isoprenoid skeleton of the terpenes can be important here. When we look at Scheme 1 it turns out that the terpenes differ mainly in the region of E ring, which is cyclopentane in lupeol and cyclohexane in amyrins. Lupeol has the isopropene substituent at C19 carbon atom of ring E; whereas amyrins differ in the methyl groups substituted at C19 and C20 in AMalf and both at C20 in AMbet. The isopropene substituent in lupeol is bigger than the methyls in amyrins and can be considered a steric hindrance. However, the sign of ΔG^{exc} for the systems with lupeol is negative and for the systems with amyrins positive, so the interactions of ECCL and ECPG with lupeol are energetically favorable and with amyrins unfavorable. Therefore, the difference in interactions with *E. coli* lipids is not connected with the substituents of the E ring of the investigated terpenes. Thus, the chiral effects can be more important here. The effects can be connected both with the structure of the terpenes and with the structure of *E. coli* CL. All five rings in the structure of lupane-type terpenes are *trans*-fused; whereas the connection between ring D and E in amyrins has the *cis* conformation. The fused rings of lupeol lie approximately in one-plane, whereas the *cis* connection produces a puckered shape at that ring junction [6]. Thus, the *cis* junction between rings D and E together with methyl groups substituted to ring E can be considered the steric hindrance which interacting with the cyclopropane ring of the cyclo-17:0 fatty acid rest makes the interactions between amyrins and ECCL and ECPG energetically unfavorable. As it was mentioned above the chiral effects can also be connected with the ECCL molecule. The middle carbon atom (C2) in the connecting headgroup glycerol in cardiolipins is protochiral [38]. It means that if the cardiolipin is symmetrically substituted as are TOCL and BHCL this center is achiral, but if CL is not symmetrically substituted as is ECCL this center is chirally active and additional chiral interactions can occur in multicomponent systems. This interaction can be responsible for the differences in the interactions with *E. coli* lipids observed for AMalf and AMbet. AMalf has 10 chiral carbon atoms and AMbet has 8, so it is possible that in the interaction with ECCL the chiral recognition is important.

In the discussion in the previous sections we focused our attention mainly on the interactions between the investigated terpenes and cardiolipins, as in mitochondria, PGs are rather minor components of the membrane. Moreover, our results indicated that the terpenes cannot disturb the PG-reach regions of the membrane. Here discussing the lipids of *E. coli* we should pay much attention to the results with ECPG, as PGs are much more populated in bacterial membranes than CLs. Our results indicate that regarding the ΔG^{exc} criterion and taking into consideration the BAM images lupeol does not have a great potential to disintegrate the organization of bacterial anionic lipids. In this point our model is in accordance with the scientific literature as most clinical and pharmacological papers regarding lupeol report its anticancer and not its antibacterial activity. Anticancer activity is connected with the mitochondrial cardiolipins, whereas antibacterial with bacterial anionic lipids. Vice versa, amyrins are reported in the literature as potent antimicrobial agents, but their anticancer activity seems to be much lower as compared with lupeol or oxidized pentacyclic terpenes.

4. Conclusions

The results of experiments reported in multiple medical and pharmaceutical publications pointed out that the molecular mechanism of biological activity of pentacyclic triterpenes may be membrane-related [13,55] and that the interactions of these compounds with anionic phospholipids: cardiolipins and phosphatidylglycerols may be highly important in this context [49]. This motivated our experiments in which binary Langmuir monolayers composed of the selected anionic phospholipids and triterpenes were used as comprehensive, reduced models of lipid matrices. We applied two mitochondrial CLs: BHCL — the widest populated mitochondrial cardiolipin, TOCL — main cardiolipin of human lymphoblasts and ECCL — cardiolipin isolated from *E. coli* membranes [37,39]. Two PGs: DLPG and DOPG are correlated with BHCL and TOCL, respectively, and were investigated for comparison purposes as PGs are found only in minor amounts in mitochondrial membranes. In contrast ECPG, a PG extracted from *E. coli*, is one of the main components of its membrane, so the investigation of its binary mixtures with pentacyclic triterpenes was crucial for the understanding of the antibacterial activity of the investigated terpenes. It turned out that the mitochondrial cardiolipins BHCL and TOCL do not discriminate over the investigated terpenes, as the results were qualitatively similar. In all binary systems containing BHCL or TOCL and the PT the sign of ΔG^{exc} was positive. Positive sign of ΔG^{exc} indicates that the interactions of the components of binary mixtures are energetically unfavorable as compared to reference one-component monolayers [47]. We interpreted the positive values of ΔG^{exc} as the indicator of the disintegration potency of the terpenes. The higher the value of ΔG^{exc} the higher is the potential of the particular terpene to disintegrate the organization of anionic phospholipids in the membrane. BHCL is the most representative mitochondrial CL among eukaryotes. In systems with BHCL the highest values of ΔG^{exc} were observed for α-amyrin, so this compound can be treated as the most potent mitochondrial toxin from the ones investigated. On the other hand, in systems with TOCL the highest ΔG^{exc} values were noticed for the mixtures with lupeol. TOCL is the main mitochondrial CL in lymphoblasts [37] so lupeol can be the terpene of choice in the therapies of some kinds of leukemia. In the studies regarding bacterial phospholipids extracted from *E. coli* it turned out that also α-amyrin has the highest potential of the disintegration of bacterial CL

and PG order. Multiple papers reported the antibacterial activity of amyrins [23–25]; however, most frequently both amyrins were investigated together. Our model studies indicate that α-amyrin is more effective in its interactions with bacterial CLs and PGs than its isomer β-amyrin. The bacterial anionic phospholipids ECCL and ECPG exhibited the possibility to discriminate over the investigated triterpenes, as the results for them were qualitatively mutually different. We tried to elucidate the observed differences taking into consideration the phenomenon of chiral discrimination. All the rings in lupeol skeleton have the junctions in *trans* configuration which makes the system of condensed rings virtually flat, whereas one *cis* junction present in amyrins between rings D and E deviates the fused ring system from planarity. Additionally the amyrins differ mutually in the number and location of chiral centers. The most important element of ECCL structure, which can lead to the discrimination over the terpenes, is the cyclopropane ring present in one of the CL fatty acid chains. Another important factor can be the presence of one additional chiral center on the C2 carbon atom in the middle glycerol moiety in ECCL structure [38]. This carbon atom is achiral in BHCL and TOCL. The studies performed on simple model systems shed new light on the interaction of pentacyclic triterpenes with anionic phospholipids on the molecular level and the binary Langmuir monolayers, for which our studies were performed, are good starting point for further investigations on more complex artificial membrane systems.

Acknowledgement

This project was financed by the National Science Centre (No. DEC-2012/05/B/ST5/00287).

The research was carried out with the equipment (UltraBAM) purchased thanks to the financial support of the European Regional Development Fund in the framework of the Polish Innovation Economy Operational Program (contract no. POIG.02.01.00-12-023/08).

Appendix A. Supplementary data

Supplementary data to this article can be found online at http://dx.doi.org/10.1016/j.bbamem.2014.05.009.

References

[1] M.N. Laszczyk, Pentacyclic triterpenes of the lupane, oleanane and ursane group as tools in cancer therapy, Planta Med. 75 (2009) 1549.
[2] G. Brezesinski, D. Vollhardt, Model studies of the interfacial ordering of oleanolic acid in the cuticula, ChemPhysChem 9 (2008) 1670.
[3] S. Alakurtti, T. Makela, S. Koskimies, J. Yli-Kauhaluoma, Pharmacological properties of the ubiquitous natural product botulin, Eur. J. Pharm. Sci. 29 (2006) 1.
[4] F.W.A. Barros, P.N. Bandeira, D.J.B. Lima, A.S. Meira, S.S. de Fanas, M.R.J.R. Albuquerque, H.S. dos Santos, T.L.G. Lemos, M.O. de Morais, L.V. Costa-Lotuto, C. do O Pessoa, Amyrin esters induce cell death by apoptosis in HL-60 leukemia cells, Bioorg. Med. Chem. 19 (2011) 1268.
[5] S. Jager, H. Trojan, T. Kopp, M. Laszczyk, A. Scheffler, Pentacyclic triterpene distribution in various plants — rich sources for a new group of multi-potent plant extracts, Molecules 14 (2009) 2016.
[6] D.W. Nes, E. Heftmann, A comparison of triterpenoids with steroids as membrane components, J. Nat. Prod. 44 (1981) 377.
[7] E. Breitmaier, Terpenes, Wiley-VCH, Weinheim, 2006.
[8] R.S. Correa, C.P. Coelho, M.H. dos Santos, J. Ellena, A.C. Doriguetto, Lupeol, Acta Crystallogr. C 65 (2009) o97.
[9] K. Surendra, E.J. Corey, A short enantioselective total synthesis of the fundamental pentacyclic triterpene lupeol, J. Am. Chem. Soc. 131 (2009) 13928.
[10] C.C. Zhao, J.H. Shao, J.D. Fan, A new triterpenoid with antimicrobial activity from *Anemone rivularis*, Chem. Nat. Compd. 48 (2012) 803.
[11] M.B.C. Gallo, M.J. Sarachine, Biological activities of lupeol, Int. J. Biomed. Pharm. Sci. 3 (2009) 46.
[12] P.K. Chaturvedi, K. Bhui, Y. Shukla, Lupeol: connotations for chemoprevention, Cancer Lett. 263 (2009) 1.
[13] M. Saleem, Lupeol, a novel anti-inflammatory and anti-cancer dietary triterpene, Cancer Lett. 285 (2009) 109.
[14] N. Nuraje, H. Bai, K. Su, Bolaamphiphilic molecules: assembly and applications, Prog. Polym. Sci. 38 (2013) 302.
[15] X.L. Sun, N. Biswas, T. Kai, Z. Dai, R.A. Dluhy, E.L. Chaikof, Membrane-mimetic films of asymmetric phosphatidylcholine lipid bolaamphiphiles, Langmuir 22 (2006) 1201.
[16] M. Broniatowski, M. Flasiński, P. Wydro, Lupane-type pentacyclic triterpenes in Langmuir monolayers: a synchrotron radiation scattering study, Langmuir 28 (2012) 5201.
[17] M. Saleem, S. Kaur, M.H. Kweon, V.M. Adhami, F. Afaq, H. Mukhtar, Lupeol, a fruit and vegetable based triterpene, induces apoptotic death of human pancreatic adenocarcinoma cells via inhibition of Ras signaling pathway, Carcinogenesis 26 (2005) 1956.
[18] M. Saleem, A. Alam, S. Arifin, M.S. Shah, B. Ahmed, S. Sultana, Lupeol, a triterpene, inhibits early responses of tumor promotion induced by benzoyl peroxide in murine skin, Pharmacol. Res. 43 (2001) 127.
[19] M. Saleem, N. Maddodi, M.A. Zaid, N. Khan, B. bin Hafeez, M. Asim, Y. Suh, J.M. Yun, V. Setaluri, H. Mukhtar, Lupeol inhibits growth of highly aggressive human metastatic melanoma cells in vitro and in vivo by inducing apoptosis, Clin. Cancer Res. 14 (2008) 2119.
[20] M. Saleem, I. Murtaza, R.S. Tarapore, Y. Suh, V.M. Adhami, J.J. Johnson, I.A. Siddiqui, N. Khan, M. Asim, B.B. Hafeez, M.T. Shekhani, B. Li, H. Mukhtar, Lupeol inhibits proliferation of human prostate cancer cells by targeting β-catenin signaling, Carcinogenesis 30 (2009) 808.
[21] R. Medeiros, M.F. Otuki, M.C.W. Avellar, J.B. Calixto, Mechanisms underlying the inhibitory actions of the pentacyclic triterpene α-amyrin in the mouse skin inflammation induced by phorbol ester 12-O-tetradecanoylphorbol-13-acetate, Eur. J. Pharmacol. 559 (2007) 227.
[22] S.A. Holanda Pinto, L.M.S. Pinto, G.M.A. Cunha, M.H. Chaves, F.A. Santos, V.S. Rao, Anti-inflammatory effect of α, β-amyrin, a pentacyclic triterpene from *Protium heptaphyllum* in rat model of acute periodontitis, Inflammopharmacology 16 (2008) 48.
[23] P.Y. Chung, P. Navaratnam, L.Y. Chung, Synergistic antimicrobial activity between pentacyclic triterpenoids and antibiotics against *Staphylococcus aureus* strains, Ann. Clin. Microbiol. Antimicrob. 10 (2011) 25.
[24] G. Diaz-Ruiz, L. Hernandez-Vazquez, H. Luna, M.C. Wacher-Rodarte, A. Navarro-Ocana, Growth inhibition of *Streptococcus* from the oral cavity by α-amyrin esters, Molecules 17 (2012) 12603.
[25] P.Y. Chung, L.Y. Chung, P. Navaratham, Transcriptional profiles of the response of methicillin-resistant *Staphylococcus aureus* to pentacyclic triterpenoids, PLoS ONE 8 (2013) e56687.
[26] V. Sudhahar, S.A. Kumar, P. Varalakshmi, Role of lupeol and lupeol linoleate on lipemic-oxidative stress in experimental hypercholesterolemia, Life Sci. 78 (2006) 1329.
[27] V. Sudhahar, S.A. Kumar, P. Varalakshmi, V. Sujatha, Protective effect of lupeol and lupeol linoleate in hypercholesterolemia associated renal damage, Mol. Cell. Biochem. 317 (2008) 11.
[28] J.F. Vasconcelos, M.M. Teixeira, J.M. Barbosa-Filho, A.S.S.C. Lucio, J.R.G.S. Almeida, L.P. de Queiroz, R. Ribeiro-dos-Santos, M.B.P. Soares, The triterpenoid lupeol attenuates allergic airway inflammation in a murine model, Int. Immunopharmacol. 8 (2008) 1216.
[29] A. Almeida Santos, J. Torres Frota, B. Rodriguez Arruda, T. Sousa de Melo, A.A. de Carvalho Almeida da Silva, G.A. Castro Brito, M.H. Chaves, V.S. Rao, Antihyperglycemic and hypolipidemic effects of α, β-amyrin, a triterpenoid mixture from *Protium heptaphyllum* in mice, Lipids Health Dis. 11 (2012) 98.
[30] T. Akihisa, S.G. Franzblau, M. Uriva, H. Okuda, F. Zhang, K. Yasukawa, T. Suzuki, Y. Kimura, Antitubercular activity of triterpenoids from Asteraceae flowers, Biol. Pharm. Bull. 28 (2003) 158.
[31] J. Fotie, D.S. Bohle, M.L. Leimanis, E. Georges, G. Rukunga, A.E. Nkengfack, Lupeol long-chain fatty acid esters with antimalarial activity from *Holarrhena floribunda*, J. Nat. Prod. 69 (2006) 62.
[32] N. Nigam, S. Prasad, J. George, Y. Shulda, Preventive effects of lupeol on DMBA induced DNA alkylation damage in mouse skin, Biochem. Biophys. Res. Commun. 381 (2009) 253.
[33] R.M. Epand, S. Rotem, A. Mor, B. Bemo, R.F. Epand, Bacterial membranes as predictors of antimicrobial potency, J. Am. Chem. Soc. 130 (2008) 14246.
[34] R.F. Epand, P.B. Savage, R.M. Epand, Bacterial lipid composition and the antimicrobial efficacy of cationic steroid compounds (Ceragenins), Biochim. Biophys. Acta Biomembr. 1768 (2007) 2500.
[35] F. Cronier, A. Patenaude, R.C. Gaudreault, W. Auger, Membrane composition modulates the interaction between a new class of antineoplastic agents deriving from aromatic 2-chloroethylureas and lipid bilayers: a solid-state NMR study, Chem. Phys. Lipids 148 (2007) 125.
[36] M. Schlame, D. Rua, M.L. Greenberg, The biosynthesis and functional role of cardiolipin, Prog. Lipid Res. 39 (2000) 257.
[37] M. Schlame, S. Brody, K.Y. Hostetler, Mitochondrial cardiolipin in diverse eukaryotes. Comparison of biosynthetic reactions and molecular acyl species, Eur. J. Biochem. 212 (1993) 727.
[38] M. Schlame, M. Ren, Y. Xu, M.L. Greenberg, I. Haller, Molecular symmetry in mitochondrial cardiolipins, Chem. Phys. Lipids 138 (2005) 38.
[39] T.A. Garrett, A.C. O'Neill, M.L. Hopson, Quantification of cardiolipin molecular species in *Escherichia coli* lipid extracts using liquid chromatography/electrospray ionization mass spectrometry, Rapid Commun. Mass Spectrom. 26 (2012) 2267.
[40] S. Sennato, F. Bordi, C. Cametti, C. Coluzza, A. Desideri, S. Rufini, Evidence of domain formation in cardiolipin-glycerophospholipid mixed monolayers. A thermodynamic and AFM study, J. Phys. Chem. B 109 (2005) 15950.
[41] O. Demenech, L. Redondo, M.T. Montero, J.H. Hernandez-Borrel, Specific adsorption of cytochrome c on cardiolipin-glycerophospholipid monolayers and bilayers, Langmuir 23 (2007) 5651.

[42] P.H.B. Aoki, D. Volpati, W. Caetano, C.J.L. Constantino, Study of the interaction between cardiolipin bilayers and methylene blue in polymer-based layer-by-layer and Langmuir films applied as membrane mimetic systems, Vib. Spectrosc. 54 (2010) 93.
[43] F. Etienne, Y. Roche, P. Peretti, S. Bernard, Cardiolipin packing ability studied by grazing incidence X-ray diffraction, Chem. Phys. Lipids 152 (2008) 13.
[44] A. Shokri, G. Larsson, Characterisation of the *Escherichia coli* membrane structure and function during fedbatch cultivation, Microb. Cell Factories 3 (2009) (art. no. 9).
[45] L. Picas, C. Suarez-Germa, M.T. Montero, O. Domenech, J. Hernandez-Borrell, Miscibility behavior and nanostructure of monolayers of the main phospholipids of *Escherichia coli* inner membrane, Langmuir 28 (2012) 701.
[46] www.avantilipids.com.
[47] I.S. Costin, G.T. Barnes, Two-component monolayers II. Surface pressure–area relations for the octadecanoi docosyl sulphate system, J. Colloid Interface Sci. 51 (1975) 106.
[48] S. Nichols-Smith, S.Y. Teh, T.L. Kuhl, Thermodynamic and mechanical properties of model mitochondrial membranes, Biochim. Biophys. Acta Biomembr. 1663 (2004) 82.
[49] Y. Chen, R. Sun, B. Wang, Monolayer behavior of binary systems of betulinic acid and cardiolipin: thermodynamic analyses of Langmuir monolayers and AFM study of Langmuir–Blodgett monolayers, J. Colloid Interface Sci. 353 (2011) 294.
[50] K. Hąc-Wydro, P. Dynarowicz-Łątka, Externalization of phosphatidylserine from inner to outer layer may alter the effect of plant sterols on human erythrocyte membrane — the Langmuir monolayer studies, Biochim. Biophys. Acta Biomembr. 1818 (2012) 2184.
[51] K. Hąc-Wydro, R. Lenartowicz, P. Dynarowicz-Łątka, The influence of plant stanol (β-sitostanol) on inner leaflet of human erythrocytes membrane modeled with the Langmuir monolayer technique, Colloids Surf. B: Biointerfaces 102 (2013) 178.
[52] D.W. Grogan, J.E. Cronan Jr., Cyclopropane ring formation in membrane lipids of bacteria, Microbiol. Mol. Biol. Rev. 61 (1997) 429.
[53] J.E. Cronan Jr., Phospholipid modifications in bacteria, Curr. Opin. Microbiol. 5 (2002) 202.
[54] Y.Y. Chang, J.E. Cronan Jr., Membrane cyclopropane fatty acid content is a major factor in acid resistance of *Escherichia coli*, Mol. Microbiol. 33 (1999) 249.
[55] H.L. Ziegler, H. Franzyk, M. Sairafianpour, M. Tabatabai, M.D. Tehrani, K. Bagherzadeh, H. Hagerstrand, D. Staerk, J.W. Jaroszewski, Erythrocyte membrane modifying agents and the inhibition of *Plasmodium falciparum* growth: structure–activity relationships for betulinic acid analogues, Bioorg. Med. Chem. 12 (2004) 119.